ROBUSTNESS ANALYSIS AND OPTIMIZATION OF COUPLED POWER AND COMMUNICATION NETWORKS BASED ON NETWORK MOTIFS PARTITIONING MECHANISM

Yonggang LI[1]*, Yaotong SU[2], Lei XIA[3], Jianlin CHEN[4], Longjiang LI[5]

The smart grid, composed of the power grid and communication networks, is formed through a complex interplay between intelligent power grid technology's high-reliability operation and monitoring and control. This interaction necessitates that both systems provide electrical energy to one another. Constructing a power grid model, we apply the Louvain algorithm to detect and divide its network motif structure. Subsequently, dividing the communication network into access, backbone, and core layers is done. The partitioning mechanism with motifs maps the physical topological layout into the virtual space to create a new coupling model integrating the power and information flow. We propose a new motif-based robust optimization algorithm — MROA. By using MROA, the network robustness is evaluated and optimized. Simulation analysis was employed to validate the efficacy and practicality of this proposed strategy for analyzing and optimizing the coupled network based on its motif composition.

Keywords: power grid, communication network, simulated annealing, network motifs, coupling network, robust optimization

1. Introduction

As the study of complex systems theory and models advances, independent systems often need to integrate with and depend on other relevant systems to fulfill complex engineering requirements. Network motifs [1] are recurring identical subgraphs in networks, defined by specific interaction patterns among vertices, each reflecting a framework for a specific function. Motifs are significant because they reflect the nature of the network function. These motif structures form complex integrated entities like Cyber-Physical Systems (CPS), including protein networks, orbital networks [2], and public transportation facilities [3], and more. However,

[1] School of Communication and Information Engineering, Chongqing University of Post and Telecommunications, Chongqing, 40065, China. Corresponding author's e-mail: lyg@cqupt.edu.cn
[2] School of Communication and Information Engineering, Chongqing University of Post and Telecommunications, Chongqing, 40065, China.
[3] State Grid Chongqing Electric Power Company Electric Power Science Research Institute, Chongqing, 401121, China.
[4] School of Communication and Information Engineering, Chongqing University of Post and Telecommunications, Chongqing, 40065, China
[5] School of Informational and Communication, University of Electronic Science and Technology, Chengdu, 611731, China.

this closely coupled manner increases the possibility of faults. In recent years, numerous serious power incidents have occurred due to the occurrence of cascading failures in a specific region or equipment, affecting entire power lines or even larger power systems, resulting in significant consequences [4]. Current research focuses on constructing heterogeneous device-interconnected complexes in the power sector, simulating emergencies, and assessing dynamic and static stability and reliability [5]. Finally, a robustness evaluation is conducted on the power and communication composite model.

The dual-layer coupled network model, introduced by Buldyrev et al. in 2010 [6], explores interactions between power and communication systems, where each node has a counterpart. Simulations show that the largest connected subnet in the dual-layer coupled network experiences a first-order phase transition during cascading failures, unlike the second-order transition in non-coupled networks. This indicates reduced robustness due to interdependence. Further studies have highlighted dynamic differences between single-layer and double-layer networks [7]. In 2013, research on cascading failures in power systems suggested protective measures [8]. Neural networks have been used to assess power system stability during maintenance [9,10]. Studies also compared random and targeted attacks in complex networks [11] and investigated node safety during failures [12]. A self-coupling node model in power-communication networks allows nodes to operate independently, such as a substation with both power and communication nodes. The ratio of power to communication resources significantly impacts the network's dynamic performance [13]. While optimizing network robustness is a current research focus, the robustness of coupled characteristic networks remains understudied. Enhancing robustness is mainly achieved by adjusting topological structures [14], without fully considering system-wide robustness. A failure in one part of a coupled network can lead to the paralysis of the entire system [15]. In power and communication systems, placing vulnerable key points at critical junctions poses significant threats. Most robustness research focuses on single-point networking, not on network partitions. The motif structure reveals subnetwork relationships, and different robust optimization methods affect the motif architecture, causing partial failures in coupled systems [16]. Deep learning has been used to develop a communication network fault diagnosis model based on deep belief networks [17,18]. Research has also created a hybrid AC/DC microgrid model to analyze various fault types [19,20]. The amount of information adversaries acquire influences their attack efficiency on Cyber-Physical Systems (CPS). Accurate fault identification and decoupling are crucial for enhancing the robustness of power-communication networks under the motif structure. This paper proposes a robustness optimization method based on motif granularity for such networks.

The paper uses the Louvain technique to identify the motif architecture of

the coupled power and communication system, modeling the interaction between power and information flow to predict the dynamic evolution of coupling relationships. Conventional intelligent algorithms protect nodes and ensure stable node degrees within internal motifs, while an intelligent path replanning mechanism adjusts the coupling degree between multiple motifs. Simulation results show that the proposed algorithm significantly enhances the robustness of the power-communication network under complex interactions.

2. Coupled Modeling of Power Grid and Communication Network

The integrated power grid-communication network system combines the power grid and communication network, highlighting their interdependence. Electrical energy from the power grid is used by the communication network for data transmission. The communication network has three layers: access, backbone, and core. The access layer includes terminal substations and nearby backbone nodes, often near power generation sites. The backbone layer consists of fiber optic lines connecting 220kV substations, while the core layer includes primary and backup dispatch centers and 500kV substations.

2.1 Division of Power Grid Model Network Motifs

From the perspective of complex networks, we construct a power grid model by considering each electrical equipment in the power grid structure as a set of nodes $V_P = \{1, 2, \cdots, N\}$, and the transmission lines are regarded as the set of edges E_P, ultimately forming the power grid $G_P(V_P, E_P)$. The adjacency matrix $\boldsymbol{A}_P$ is used to describe the connection relationships among nodes in $G_P(V_P, E_P)$, where $\boldsymbol{A}_P(i, j) = 1$ if two nodes are connected, and $\boldsymbol{A}_P(i, j) = 0$ otherwise.

2.2 Division of Communication Network Model Motifs

First, we construct and partition motifs for the power grid structure, and then, based on these network motifs, we progressively build the model for the power-communication network layer by layer.

Modularity measures the quality of community structure in a network, commonly used in graph theory and network science to detect and evaluate communities. We use the Louvain algorithm [22] to extract motifs from the power system, which involves two steps: optimizing modularity and achieving network motif cohesion. The decision to continue iterative and integration operations depends on the degree of modularity improvement. We adopt the definition of modularity from reference [23]:

$$Q = \frac{1}{2m} * \sum_{ij} \left[A_{i,j} - \frac{K_i * K_j}{2m} \right] * \delta(C_i, C_j) \tag{1}$$

Where m represents the number of network connecting edges; $A_{i,j}$ is the weight of

the connecting edge in the network; K_i is the sum of the weights of connecting edges associated with node i; K_j is the sum of the weights of connecting edges associated with node J. If nodes i and J are part of the same motif, then $\delta(C_i, C_j) = 1$; otherwise, $\delta(C_i, C_j) = 0$.

When a node leaves its initial motif and migrates to another, it changes the network architecture and affects modularity, with the gain from the motif change denoted as ΔQ. By moving node i from its initial motif to the motif near node j, the gain is calculated using the following formula ΔQ:

$$\Delta Q = \left[\frac{\sum_{in} + k_{i,in}}{2m} - \left(\frac{\sum_{tot} + k_i}{2m}\right)^2 \right] - \left[\frac{\sum_{in}}{2m} - \left(\frac{\sum_{tot}}{2m}\right)^2 - \left(\frac{k_i}{2m}\right)^2 \right] = \frac{1}{2m}\left(k_{i,in} - \frac{\sum_{tot} k_i}{2m}\right) \tag{2}$$

Here, $\sum_{in}$ is the sum of connection weights within the motif; $\sum_{tot}$ is the sum of connection weights outside the motif; the degree of node i is k_i; the degree from i to the internal motif is $k_{i,in}$; and m is the sum of all link weights. If $\Delta Q < 0$, no action is taken; otherwise, motif ownership and numbering are adjusted. This continues until the network structure is stable and modularity no longer increases. If ΔQ differs from $\max \Delta Q$ by no more than $1/2m$, the adjusted nodes overlap. The motif partitioning follows these steps:

Step 1: Designate each node as a single motif, with the total number of nodes equaling the total number of motifs.

Step 2: Node migration between motifs: Transfer each node one by one to nearby motifs, calculating the change in ΔQ before and after migration. If the migration results in the greatest change, the migration is successful; otherwise, the state remains unchanged.

Step 3: Execute Step 2. For each node in the network, move it according to the method in Step 2 until there is no further change in the motif.

Step 4: Reconstruct motifs. Consider the weights of nodes within motifs as the weights of the new node rings, and also consider the weights of inter-motif connecting edges as the weights of the new node edges.

Step 5: Treat the reconstructed motifs as nodes and repeat the process in Step 2, integrating motifs until their modularity gain does not change further.

2.3 Communication Network Access Layer Model

The communication access layer is within the substations, and its layout mirrors the power grid's pattern. There is a significant similarity between the hierarchical structure of the electrical network in the substations and the communication network. The topological structures of the communication network

and the power grid are denoted as $G_{c1}(V_{c1}, E_{c1})$ and $G_p(V_p, E_p)$, respectively. The number of nodes and the network structure closely resemble or are identical to those of the distribution substations:

$$G_{c1}(V_{c1}, E_{c1})=G_p(V_p, E_p) \tag{3}$$

$$\boldsymbol{A}_{c1} = \boldsymbol{A}_p \tag{4}$$

Where $\boldsymbol{A}_{c1}$ represents the communication adjacency matrix, and this adjacency matrix is directly coupled on a one-to-one basis with the power grid.

2.4 Communication Network Backbone Layer Model

Data transmission and control systems are integral to the data communication network, showing clear motif aggregation. Thus, when modeling the communication backbone layer, node motifs must be allocated first, followed by establishing motif topology [24-25].

The core node motifs are the primary consideration, with the weighted modularity function value Q as the objective. Core nodes serve as motif centers, and the relationships between backbone points and motif ownership are optimization variables. This leads to the following model:

1) Objective Function

$$\begin{cases} \max Q = \sum_{a=1}^{n} \frac{1}{2m} \sum_{i,j \in a} \left[\boldsymbol{A}_w(i,j) - \frac{k_i k_j}{2m} \right] \tau_{a,i} \tau_{a,j} \\ k_i = \sum_{j=1}^{n} \boldsymbol{A}_w(i,j) \\ m = \sum_{i,j}^{n} \boldsymbol{A}_w(i,j)/2 \end{cases} \tag{5}$$

Here, n is the number of motifs, $\tau_{a,i}$ represents whether a node i is assigned to a motif a, in which case $\tau_{a,i}$=1; otherwise, $\tau_{a,i}$=0; m is the sum of weights; $\boldsymbol{A}_w$ is the adjacency weight matrix. We express it by combining the degree of coupling between power and communication and the length of connections between nodes. Each element of $\boldsymbol{A}_w$ is defined as follows:

$$\boldsymbol{A}_w(i,j) = (\boldsymbol{E}_p(i,j) \times l_{(i.j)})^{-1} \tag{6}$$

2) Constraints

Constraint on Single Ownership of Motif for Backbone Layer Nodes:

$$\sum_{i=1}^{n} \tau_{a,i} = 1 \quad \forall a = 1, 2, \cdots, n \tag{7}$$

Constraint on the Number of Backbone Nodes within a Motif:

$$n_{\min} < \sum_{i=1}^{n} \tau_{a,i} < n_{\max} \quad \forall a = 1, 2, \cdots, n \tag{8}$$

Where $n_{\min}$ and $n_{\max}$ are the upper and lower limits, respectively, on the number of internal nodes within a motif.

For constructing motifs in the communication layer, $G_{c2}(V_{c2}, E_{c2})$ is considered the topology graph of the backbone layer, with its adjacency matrix defined as $\boldsymbol{A}_{c2}$. Inter-layer connections, such as those between the backbone and access layers, follow a one-to-many pattern.

2.5 Communication Network Core Layer Model

The communication system's core layer typically uses high-end routers, with some main nodes directly connected to backup points. Core nodes intersect with backbone nodes, forming a many-to-many connection. The constructed topology for the core is denoted as $G_{C_3}(V_{C_3}, E_{C_3})$, with $\boldsymbol{A}_{C3}$ as the adjacency matrix, showing the connections between core and backbone nodes.

2.6 Coupled Network Model of Power Grid and Communication Network

We define the strong-weak coupling network model $G_{pc}(V_{pc}, E_{pc})$ for the power grid and communication network, with $\boldsymbol{A}_{pc}$ serving as the adjacency matrix defined as follows:

$$\boldsymbol{A}_{pc} = \begin{bmatrix} \boldsymbol{A}_{p-p} & \boldsymbol{A}_{p-c1} & 0 & 0 \\ \boldsymbol{A}_{c1-p} & \boldsymbol{A}_{c1-c1} & \boldsymbol{A}_{c1-c2} & 0 \\ 0 & \boldsymbol{A}_{c2-c1} & \boldsymbol{A}_{c2-c2} & \boldsymbol{A}_{c2-c3} \\ 0 & 0 & \boldsymbol{A}_{c3-c2} & \boldsymbol{A}_{c3-c3} \end{bmatrix} \tag{9}$$

In Equation (9), $\boldsymbol{A}_{p-c1}, \boldsymbol{A}_{c1-p}, \boldsymbol{A}_{c1-c2}, \boldsymbol{A}_{c2-c1}, \boldsymbol{A}_{c2-c3}, \boldsymbol{A}_{c3-c2}$ represent different types of coupling matrices, such as $\boldsymbol{A}_{p-c1}$ being the coupling matrix between the power layer and the communication access layer. Through the above calculations, the coupled model of the power-communication network, as shown in Fig. 1, can be established.

Using the Louvain algorithm, motifs are extracted from the power grid and communication network, and the network is hierarchically divided based on these motifs, ensuring the accuracy of the layered model. This model aids in understanding the dynamic coupling between power and information flow and is crucial for optimizing motif robustness. It allows consideration of each layer's characteristics during optimization, enhancing overall network robustness.

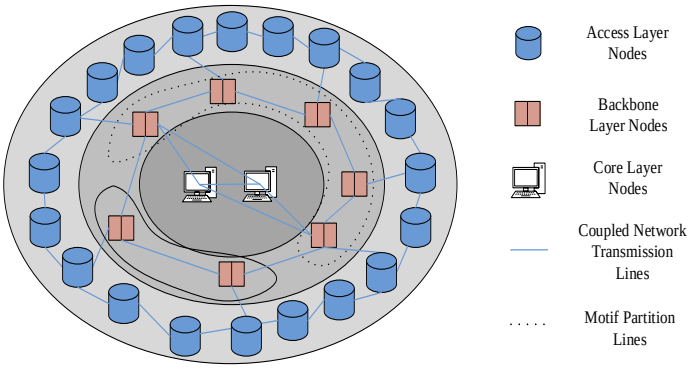

Fig.1. Coupling the power grid with the communication network based on motif structure

3. Power-Communication Coupled Network Robustness

3.1 Objective Function

Penetration probability is a crucial metric for evaluating system stability [26]. Once the system is saturated with damage, the entire system collapses. However, percolation models often overlook cases where the system sustains minor damage without a complete breakdown. For instance, the disconnection of a node or edge can change the system's structure, dividing it into isolated motifs that still maintain integrity and function [27]. A novel evaluation metric, denoted as R, has been proposed to assess network resilience against attacks [28]. Robustness R is defined as:

$$R=\frac{1}{N}\sum_{q=1}^{N}\frac{S(q)}{N} \tag{10}$$

Where $S(q)$ is defined as the maximum dimension of the largest connected subgraph after removing q nodes, and the original number of nodes is N, $R\in[1/N,0.5]$. A smaller R indicates poorer robustness.

3.2 MROA Algorithm Description

The motif structure illustrates the layout and connectivity of micro-networks. Malicious damage can compromise the motif structure, and optimizing network robustness may alter it, causing the disappearance of functional components. Thus, an appropriate optimization strategy is crucial. We propose using the motif structure to optimize the robustness of coupled power and communication systems. To preserve the original motif structure, we use normalized mutual information (NMI) [29] to assess motif modeling accuracy. The NMI standard evaluates how well the optimization scheme maintains the initial motifs. Assuming the current network with motifs is denoted as α and the optimized network as β, NMI is calculated as follows [30]:

$$N_{NMI}(\alpha,\beta)=\frac{-2\sum_{l=1}^{C_\alpha}\sum_{j=1}^{C_\beta}\boldsymbol{F}_{ij}\log_a\frac{\boldsymbol{F}_{ij}N}{\boldsymbol{F}_i\boldsymbol{F}_j}}{\sum_{i=1}^{C_\alpha}\boldsymbol{F}_i\log_a\frac{\boldsymbol{F}_i}{N}+\sum_{j=1}^{C_\beta}\boldsymbol{F}_j\log_a\frac{\boldsymbol{F}_j}{N}} \tag{11}$$

In Equation (11), C_α and C_β are the numbers of motifs before and after optimization, respectively, $\boldsymbol{F}$ is the confusion matrix. If motifs i and j are present in networks α and β, the confusion matrix is defined as $\boldsymbol{F}_{ij}$. When $N_{NMI}(\alpha,\beta)=1$ for networks α and β, it indicates that the motif structures before and after optimization are the same; otherwise, they are different. When the NMI value decreases, it implies a weaker preservation of the original motif structure. Conversely, an increase in the NMI value indicates a better preservation of the original motif structure.

To optimize the robustness metric R, we propose the Path Relinking Algorithm, which reconnects failed edges while maintaining the node degrees to enhance the resilience within motifs. Unlike the existing random rewiring (Fig. 2.a), our Path Relinking Algorithm makes slight adjustments to some edges without changing the node degrees and the network structure, as illustrated in Fig. 2.b. In this example, edges l_{ij} and l_{mn} are replaced by edges l_{in} and l_{mj}. After this edge exchange, the motif robustness becomes R'. If the adjusted robustness R' is greater than the original robustness, i.e., $R'>R$, we keep this adjustment algorithm until the robustness R no longer improves.

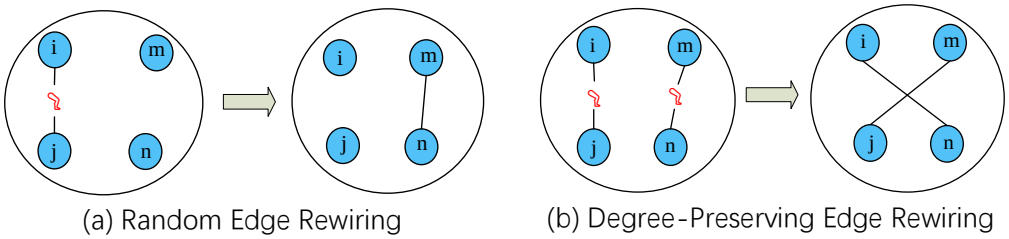

Fig.2. Two methods for reconnecting edges

As a heuristic edge rewiring algorithm, the Path Relinking Algorithm has shown good performance in optimizing network robustness. However, this method cannot completely prevent falling into local optima because it is essentially a solution based on greedy algorithms, which may overlook contradictory but superior solutions. To mitigate this, random factors should be introduced. The Simulated Annealing algorithm [31] can avoid local optima, so we propose using it.

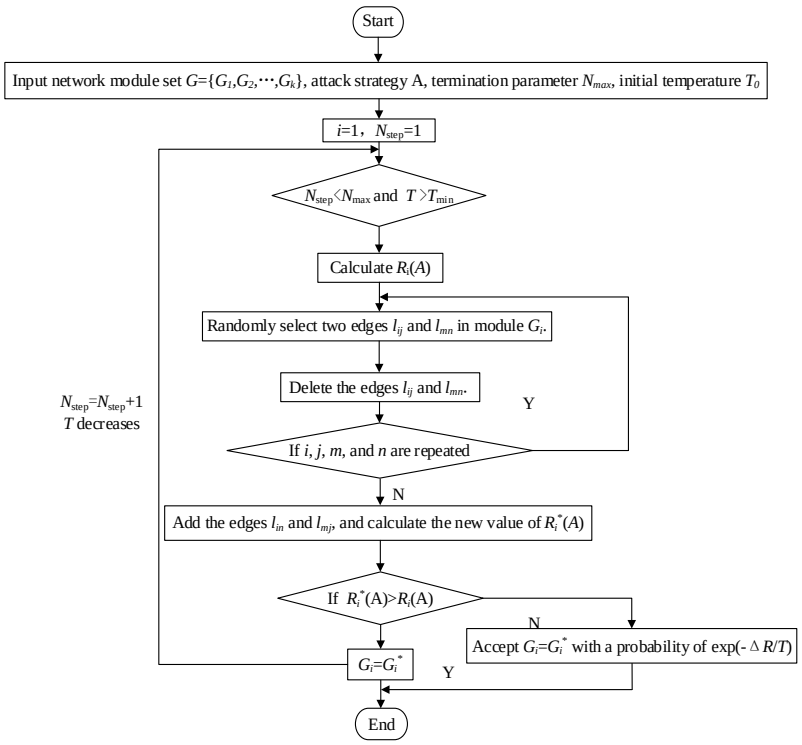

Fig.3. Motif-based degree preserving edge reconnection method based on simulated annealing

Using various disruption mechanisms A to attack a specific motif G_i, $R_i(A)$ represents the robustness post-attack. If the Path Relinking Algorithm yields motif G_i^* with robustness $R_i^*(A)$, and $R_i^*(A) \le R_i(A)$, $G_i = G_i^*$ is accepted with a certain probability. If $R_i^*(A) > R_i(A)$, the new motif G_i^* is fully accepted. The acceptance probability is influenced by $\Delta R = | R_i^* - R_i |$ and the initial temperature of the Simulated Annealing algorithm. A smaller ΔR increases rewiring success probability, while a higher initial temperature T helps avoid local optima. As iterations increase, T decreases, affecting the algorithm's performance. The change in T follows $T(i) = 0.8^i \times T^0$, where I is the iteration index. Steps for optimizing robustness within motifs using Simulated Annealing are shown in Fig. 3.

We utilize simulated annealing techniques for path relinking within motifs, optimizing robustness and observing performance differences before and after. To illustrate the algorithm's effect on the power-communication coupling network, Fig. 4 presents a simplified example with the original and optimized network structures. A specific motif from a network $G - C$ is selected to avoid affecting node degrees and robustness R. Links of two edges are cut and optimized at each level. After such operations, we obtain the new network G_{opt} and C_{opt}. It is noteworthy to note that the optimization process does not change any dependencies. Because the

optimized network has better stability than the original network nodes, it shows that the whole network system has higher stability and robustness.

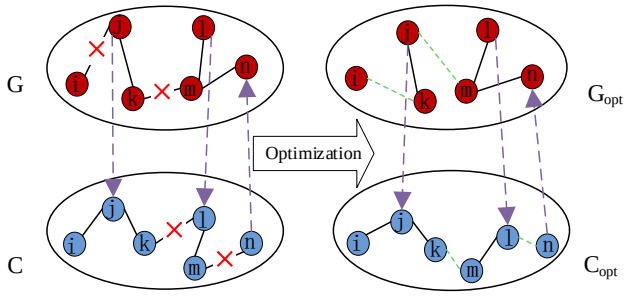

Fig.4. Schematic diagram of coupling network optimization before and after

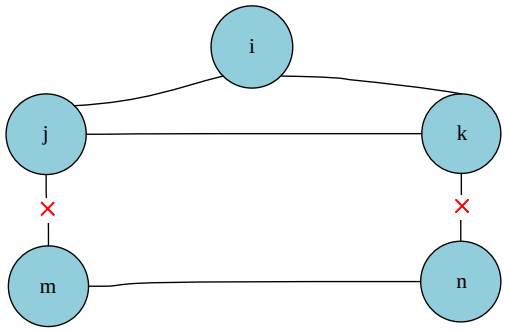

Fig.5. Intelligent rewiring algorithm

The Intelligent Rewiring Algorithm is an intelligent and efficient robustness optimization strategy [32], an improvement upon the random rewiring algorithm. As shown in Fig. 5, for a node i connected to a set of nodes, there are nodes j with an upper degree limit and nodes k with a lower degree limit. m represents the adjacent nodes of j, and n represents the adjacent nodes of k. The algorithm involves removing edges l_{jm} and l_{kn} while adding edges l_{jk} and l_{mn}. If the robustness improves, the edges l_{jk} and l_{mn} are retained; otherwise, the algorithm is re-executed with a different node i.

To enhance robustness between motifs, the intelligent rewiring algorithm is adjusted. The first step involves selecting a suitable node i with a degree $\langle k \rangle$ greater than the network's average degree. This node should be connected to at least one node outside the motif and internally connected to a node with a degree greater than 2. The second step of the algorithm, as illustrated in Fig. 6, focuses on a node j that is adjacent to node i but not in the same motif. Nodes i, m, and k are in the same motif and mutually connected. After removing edges l_{ij} and l_{km}, the algorithm switches to l_{ik} and l_{jm}. By iteratively executing multiple rounds of this

algorithm, the optimization gains in robustness between motifs can be achieved.

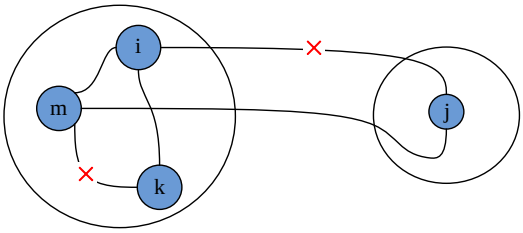

Fig.6 Method of reconnecting edges between communities

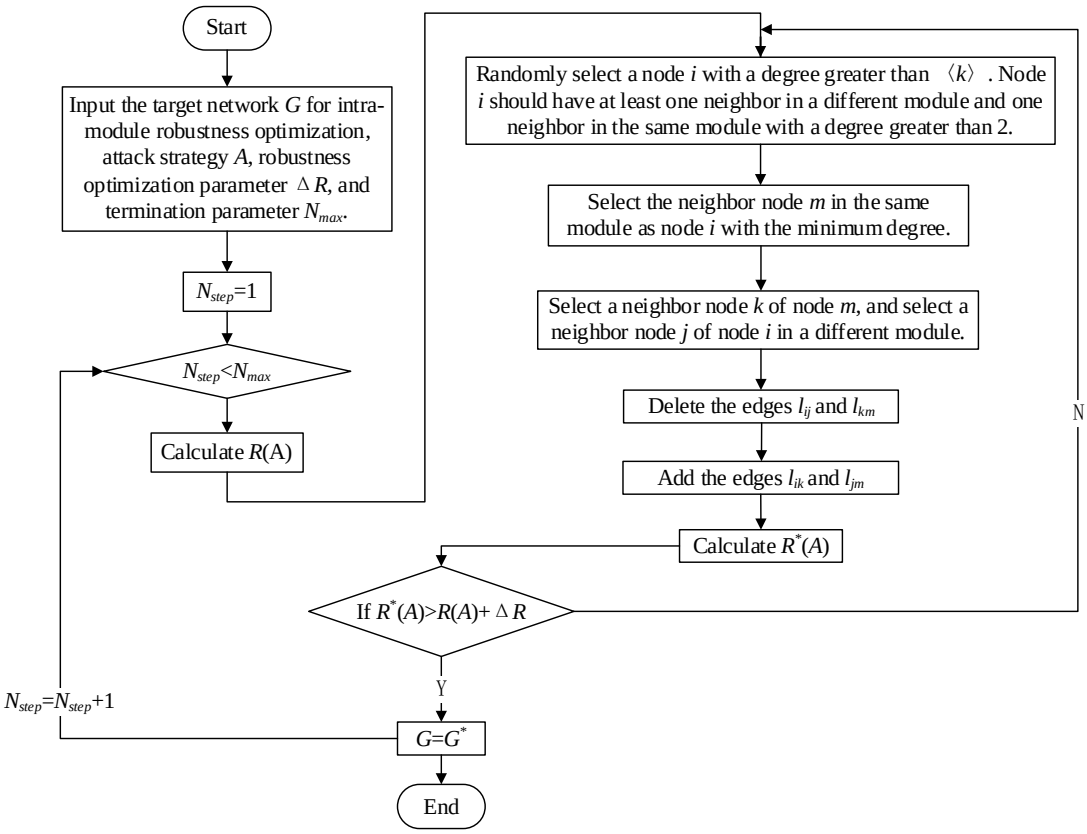

Fig.7. MROA's motif reconnection edge method based on improved intelligent rewiring policy

$R(A)$ defines the internal robustness of motifs. After the optimization, the network motif is upgraded from G to G^*, and the optimized robustness indicator is denoted as $R^*(A)$. If $R^*(A) > R(A) + \Delta R$, the current motif G is retained, achieving a single optimization. Simultaneously, a stopping threshold condition $N_{\max}$ is set to ensure the convergence of the optimization process. Fig. 7 illustrates the process flowchart of the inter-motif edge reconnection method, which is achieved by

refining the intelligent rewiring mechanism.

4. Simulation Results and Analysis

The simulation test object is IEEE-39 system. After modeling and analyzing the power communication coupling network, the power communication coupling network model is established by using MATLAB and MATPOWER.

Table 1

IEEE-39 Node Motif Division Results

Motif	Motif member	Overlapping nodes
Motif 1	1,2,4,5,6,7,8,9,11,30,31,39	4,6,11
Motif 2	4,6,10,11,12,13,14,15,32	4,6,11,15
Motif 3	3,15,16,17,18,19,20,21,24,27,33,34	15,16,17,21,24,27
Motif 4	16,21,22,23,24,35,36	16,21,24
Motif 5	17,25,26,27,28,29,37,38	17,27

Firstly, we applied the Louvain algorithm to partition the IEEE-39 system's power grid topology into motifs. Table 1 presents the predictive performance relationship over time, indicating five motifs. Fig. 8 provides a topological map with motif structures highlighted in different colors.

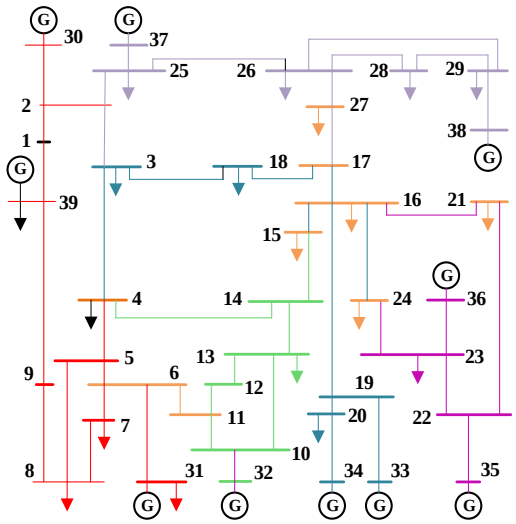

Fig.8. Schematic diagram of IEEE-39 node motif division results

The power system and its communication counterpart are partitioned into five motifs. Communication devices are organized into access, backbone, and core functional points, forming a coupled system with 39 power nodes and 50 communication nodes. The layered model architecture is shown in Fig. 9.

To improve robustness optimization efficiency, we test our models using effective attack patterns. Whether to use node-based or edge-based attacks depends on the topology. Based on relevant literature, we consider attack patterns based on

degree and betweenness centrality. Nodes are sorted by degree and betweenness centrality, and highly connected and central nodes are selected for attack and removal. These attack patterns are used to optimize motif structure robustness internally and externally. Simulation results for these attack patterns are shown in Fig. 10, with attack cycles corresponding to the number of faulty nodes.

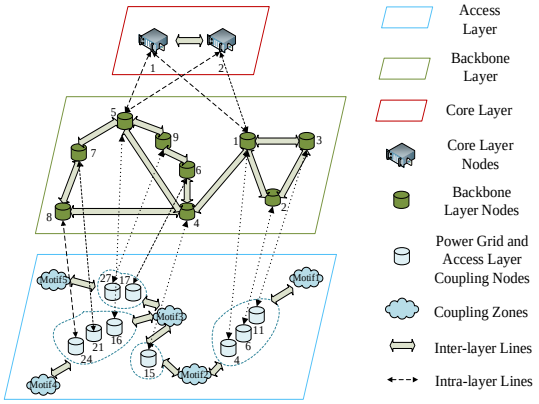

Fig.9. IEEE-39 node system coupling and layered network model

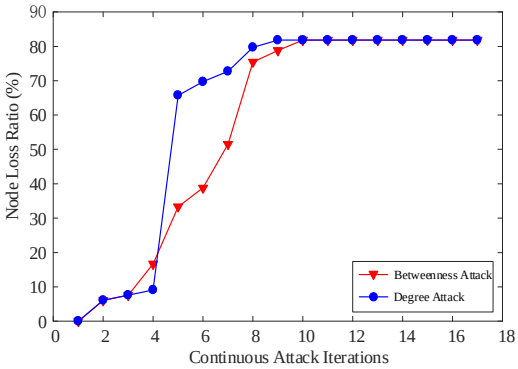

Fig.10. Robust comparison of IEEE-39 system under different attack strategies

Historically, power and communication networks have been fused one-to-one, based on node connectivity and betweenness centrality rankings. This study used the classical one-to-one coupling model and introduced a novel fusion model considering motif structures to compare robustness. The node failure ratio measures network robustness. The IEEE-39 node system is simulated by MATLAB using two methods, and the degree-based attack results are shown in Fig. 11.

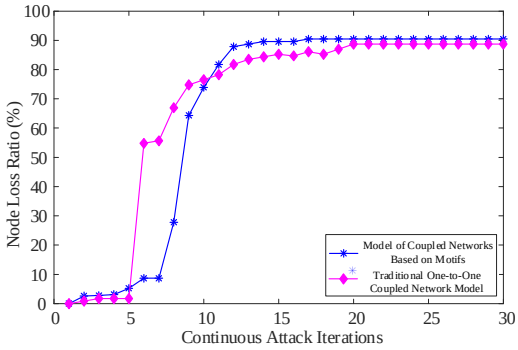

Fig.11. Comparison of Survivability of Coupled networks under different coupling modes

As shown in Fig. 11, traditional single-equation coupling of power and communication networks is prone to triggering a first-order phase transition. Attacking about 5% of nodes can cause 54.8% node failures. However, using the fusion approach based on network motif structures, a similar attack results in only 8.7% node failures. In traditional 1:1 coupling, sparse interconnections can lead to complete network breakdown, forming multiple subnets and causing significant disruption. During subsequent attacks, the isolation between subnets prevents fault spread, resulting in slower node loss growth.

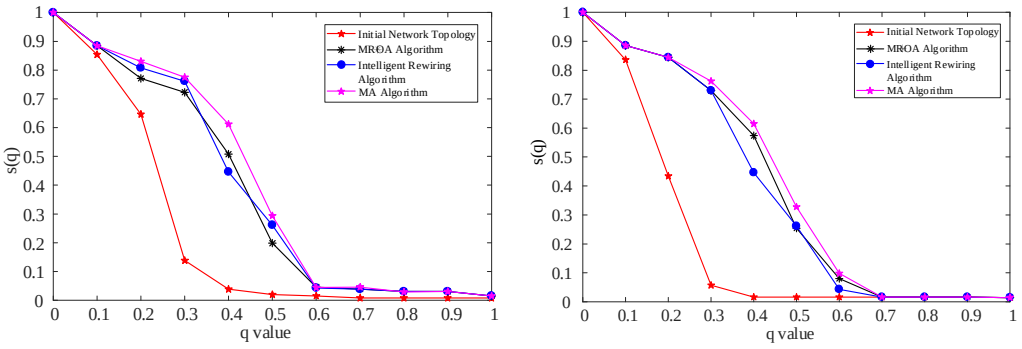

(a) Degree Attack (b) Betweenness Attack

Fig.12. Changes in s(q) of coupled networks under different optimization strategies

The simulation results of $s(q)$ for the optimized algorithm considering the motif structure of the coupled networks are shown in Fig. 12. We improved the original network motif structure while maintaining its stability, applied the proposed model to the IEEE-39 node system, and compared it with intelligent rewiring [32] and the Memetic Algorithm (MA) [33]. The MA algorithm combines genetic algorithms' global search capability with local search's fine optimization ability, effectively solving complex problems. We simulated betweenness and degree attacks on the IEEE-39 system, observed the decrease in $s(q)$ with increasing node failure rate q, and evaluated the robustness of the optimized power

and communication network coupling system.

In Fig. 12, as the parameter q increases, both attack modes show a similar trend in $s(q)$ with a conservative optimization strategy due to the IEEE-39 node coupling system's scale-free nature with a power-law degree distribution. Both attack modes accurately identify critical points, leading to similar effects. However, with intelligent rewiring and MA algorithms, the decrease in $s(q)$ is slower, and $s(q) < 0.1$ when $q = 0.6$. The MROA algorithm's $s(q)$ lies between the two. This study applied three optimization methods to the coupled power and communication network system over 10 rounds, with results in Table 2. R_{org} represents unoptimized robustness, R_{avg} is robustness after 10 optimizations, and ΔR is the improvement percentage. As shown in Table 2, under degree attacks, MROA improves network robustness by up to 61.02%. Under betweenness attacks, it achieves up to 79.31% improvement. It outperforms the intelligent rewiring scheme and is comparable to the MA algorithm's performance.

Table 2

Results of Robustness Optimization under Different Attack Strategies

	Optimization algorithm	R_{org}	R_{avg}	ΔR
Degree Attack	MROA Algorithm	0.254	0.409	0.155
	Intelligent Rewiring Algorithm	0.254	0.406	0.152
	MA Algorithm	0.254	0.428	0.174
Betweenness Attack	MROA Algorithm	0.232	0.416	0.184
	Intelligent Rewiring Algorithm	0.232	0.403	0.171
	MA Algorithm	0.232	0.432	0.200

This study used the Louvain algorithm to examine the stability of the initial modular structure in coupled power and communication networks before and after applying three robustness optimization schemes. It explored changes in Normalized Mutual Information (NMI) values during optimization, comparing the impact of these schemes on modular structure constancy.

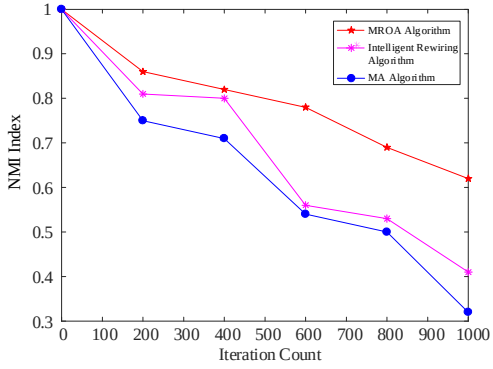

Fig.13. NMI comparison of three algorithms

Simulation results in Fig. 13 show that after 1000 iterations, the NMI index for intelligent rewiring is about 0.4, MA's NMI is around 0.3, while the proposed

modular structure algorithm achieves an NMI of about 0.6, outperforming both. We conducted 10 optimization iterations using three methods on the coupled power and communication network systems, with results presented in Table 3. N1 represents the mean constancy of the network modular structure after optimization, and N2 indicates the improvement index of the modular constancy.

From Table 3, our approach enhances the constancy of the modular structure more effectively than the traditional intelligent rewiring method. Compared to intelligent rewiring, the ΔNMI improvement is 51.9%. Compared to the MA algorithm, the ΔNMI improvement is 85.1%. Among the three algorithms, MROA maintains the best constancy of the initial modular structure.

Table 3

Effect of Motif Structure Preservation

Optimization algorithm	NMI_{avg}	ΔNMI
MROA Algorithm	0.559	-
Intelligent Rewiring Algorithm	0.368	0.191
MA Algorithm	0.302	0.257

After the experimental simulations and analysis, the MROA algorithm shows robustness similar to MA, both outperforming the intelligent rewiring algorithm. In terms of modular stability, MROA performs best in maintaining the initial network modular structure. The results indicate a differentiated downward trend in $S(q)$, showing that each algorithm has unique characteristics in enhancing system robustness. The intelligent rewiring algorithm integrates adjacency information and reselection of edges via greedy algorithms. The MA algorithm uses a population-based global search and individual-based local heuristic search, reconnecting edges under optimal conditions without constraints. This study calculates the network modular structure, using different intelligent algorithms for internal (simulated annealing) and external (improved intelligent rewiring) modules. The MA algorithm is closer to MROA in the $S(q)$ metric, showing greater stability. Maintaining the original modular structure's stability is crucial for improving the robustness of the coupled network. Simulation results show that the MROA algorithm excels in maintaining submodule stability while achieving robustness optimization similar to the MA algorithm.

5. Conclusion

This paper constructs a model of a coupled power grid and communication network to describe its complexity, aiming to achieve effective network motifs and maintain the stability of subnetwork motifs. The Louvain algorithm is used to discover motif structures in the coupled model. Based on this motif-based grid pattern, each level of the power grid and communication network is systematically constructed, forming a complex system model. The proposed Motif-based Robust

Optimization Algorithm (MROA) is introduced and compared through simulation with the Memetic Algorithm (MA) and the Intelligent Rewiring Algorithm. The results show that MROA achieves robustness optimization gains comparable to MA but superior to the Intelligent Rewiring Algorithm. Compared with MA, MROA enhances both the stability of subnetworks and the constancy of network motif structures without degrading network robustness. This algorithm proves its superiority in improving network robustness and stability. This motif-based analysis method provides a new perspective for the collaborative optimization of power and communication networks.

Future research directions could involve further validating the effectiveness of the MROA algorithm on larger-scale systems and considering network optimization problems in more practical application scenarios. Additionally, in-depth explorations of the application of motif structures in other complex systems can be undertaken to broaden the applicability of this method.

Acknowledgments

This research was funded and supported by National Key Research and Development Program of China (No. 2022YFC3005702), the Key Project of Chongqing Technology innovation & application development (Evaluation of unmanned aerial vehicle information diffusion and control technology), and the State Grid Chongqing Technology Project (2023Yudian Technology No. 32).

REFERENCES

[1] Éva Bertalan, Samo Lešnik, Urban Bren, Ana-Nicoleta Bondar, Protein-water hydrogen-bond networks of G protein-coupled receptors: Graph-based analyses of static structures and molecular dynamics, Journal of Structural Biology, 2022, 212(3): 107634.

[2] Hassiba Laifa, Raoudha khcherif, Henda Hajjami Ben Ghezalaa, Train delay prediction in Tunisian railway through LightGBM model, Procedia Computer Science, 2021, 192: 981-990.

[3] De Bona A A, de Oliveira Rosa M, Fonseca K V O, et al. A reduced model for complex network analysis of public transportation systems. *Physica A: Statistical Mechanics and its Applications*, 2021, 567: 125715.

[4] Guo H, Yu S S, Iu H H C, et al. A complex network theory analytical approach to power system cascading failure—From a cyber-physical perspective. *Chaos: An Interdisciplinary Journal of Nonlinear Science*, 2019, 29(5).

[5] Xu S, Xia Y, Ouyang M. Effect of resource allocation to the recovery of scale-free networks during cascading failures. *Physica A*: *Statistical Mechanics and its Applications*, 2020, 540: 123157.

[6] Buldyrev S V, Parshani R, Paul G, et al. Catastrophic cascade of failures in interdependent networks. *Nature*, 2010, 464(7291): 1025-1028.

[7] Gao Jianxi, Buldyrev S V, Havlin S, et al. Robustness of a network of networks. *Physical review letters*, 2011, 107(19): 195701.

[8] Huang Xuqing, Vodenska I, Havlin S, et al. Cascading failures in bi-partite graphs: model for systemic risk propagation. *Scientific reports*, 2013, 3(1): 1-9.

[9] A. Hoballah and I. Erlich, "Transient Stability Assessment Using ANN Considering Power System Topology Changes," 2009 15th International Conference on Intelligent System Applications to Power Systems, Curitiba, Brazil, 2009, pp. 1-6.

[10] Sarajcev P, Kunac A, Petrovic G, Despalatovic M. Artificial Intelligence Techniques for Power System Transient Stability Assessment. *Energies*. 2022; 15(2):507.

[11] Huang Xuqing, Vodenska I, Havlin S, et al. Cascading failures in bi-partite graphs: model for systemic

risk propagation. *Scientific reports*, 2013, 3(1): 1-9.
[12] Gao X, Peng M, Chi K T, Robustness analysis of cyber-coupled power systems with considerations of interdependence of structures, operations and dynamic behaviors. *Physica A: Statistical Mechanics and its Applications*, 2022, 596: 127215.
[13] Kong P Y, Song Y. Joint consideration of communication network and power grid topology for communications in community smart grid. *IEEE Transactions on Industrial Informatics*, 2019, 16(5): 2895-2905.
[14] Shen Y, Ren G, Ran B. Cascading failure analysis and robustness optimization of metro networks based on coupled map lattices: A case study of Nanjing, China. *Transportation*, 2021, 48(2): 537-553.
[15] Danziger, M.M., Barabási, AL. Recovery coupling in multilayer networks. *Nat Commun* **13**, 955 (2022).
[16] Mozafari M, Khansari M. Improving the robustness of scale-free networks by maintaining community structure. *Journal of Complex Networks*, 2019, 7(6): 838-864.
[17] B. Ren et al., "Research on Fault Location of Process-Level Communication Networks in Smart Substation Based on Deep Neural Networks," in IEEE Access, vol. 8, pp. 109707-109718, 2020.
[18] Rachna Vaish, U.D. Dwivedi, Saurabh Tewari, S.M. Tripathi, “Machine learning applications in power system fault diagnosis: Research advancements and perspectives,” Engineering Applications of Artificial Intelligence, Vol 106, 2021, 104504.
[19] Hossein Lotfi, Amin Khodaei, “Hybrid AC/DC microgrid planning,” Energy, Volume 118, 2017, Pages 37-46.
[20] A. M. Jasim, B. H. Jasim, V. Bureš and P. Mikulecký, "A Novel Cooperative Control Technique for Hybrid AC/DC Smart Microgrid Converters," in IEEE Access, vol. 11, pp. 2164-2181, 2023.
[21] Yiwei Zhang, Tianlun Jiang, Qingxin Shi, Wenxia Liu, Shaofeng Huang, “Modeling and vulnerability assessment of cyber physical system considering coupling characteristics,” International Journal of Electrical Power & Energy Systems, Volume 142, Part B, 2022, 108321.
[22] Ghosh S, Halappanavar M, Tumeo A, et al. Distributed louvain algorithm for graph community detection[C]//*2018 IEEE international parallel and distributed processing symposium* (IPDPS). Vancouver: IEEE Press, 2018: 885-895.
[23] Sattar N S, Arifuzzaman S. Scalable distributed Louvain algorithm for community detection in large graphs. *The Journal of Supercomputing*, 2022: 1-35.
[24] E. Cakmak, J. Fuchs, D. Jäckle, T. Schreck, U. Brandes and D. Keim, "Motif-Based Visual Analysis of Dynamic Networks," 2022 IEEE Visualization in Data Science (VDS), Oklahoma City, OK, USA, 2022, pp. 17-26.
[25] Gupta V K, Shukla D. Estimation of Average Degree of Social Network Using Clique, Shortest Path and Cluster Sampling to monitor Network Reliability. *Reliability: Theory & Applications*, 2022, 17(2 (68)): 326-339.
[26] Lorenzo Cirigliano, Gábor Timár, Claudio Castellano. Extended-range percolation in complex networks. Physical Review E, 2023, 108(4): 044304.
[27] Wan Z, Mahajan Y, Kang B W, et al. A survey on centrality metrics and their network resilience analysis. *IEEE Access,* 2021, 9: 104773-104819.
[28] Schneider C M, Moreira A A, Andrade Jr J S, et al. Mitigation of malicious attacks on networks. *Proceedings of the National Academy of Sciences*, 2011, 108(10): 3838-3841.
[29] Liu Xin, Cheng Hui Min, Zhang Zhong Yuan. Evaluation of community detection methods. *IEEE Transactions on Knowledge and Data Engineering*, 2019, 32(9): 1736-1746.
[30] Yang Zhao, Algesheimer R. Tessone C. J A Comparative analysis of community detection algorithms on artificial networks. Scientific reports, 2016, 6(1): 1-18.
[31] Gürcan Çetin, Ali Keçebaş, Optimization of thermodynamic performance with simulated annealing algorithm: A geothermal power plant, Renewable Energy, 2021, 172: 968-982.
[32] Ran Xiao. Analysis and Research of Network Robustness Based on Optimization Algorithms, 2021. (In Chinese)
[33] Ferrante Neri, Carlos Cotta, Memetic algorithms and memetic computing optimization: A literature review, *Swarm and Evolutionary Computation*, 2012, 2: 1-14.